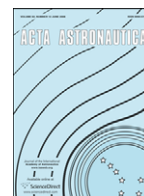




Contents lists available at ScienceDirect

Acta Astronautica

journal homepage: www.elsevier.com/locate/actaastro

A feasibility study on using inkjet technology, micropumps, and MEMs as fuel injectors for bipropellant rocket engines

Peter Glynne-Jones^a, M. Coletti^{b,*}, N.M. White^c, S.B. Gabriel^b, C. Bramanti^d

^a School of Engineering Sciences, University of Southampton, Southampton, SO17 1BJ, UK

^b Astronautics Research Group, School of Engineering Sciences, University of Southampton, Southampton, SO17 1BJ, UK

^c Electronics and Computer Science, University of Southampton, Southampton, SO17 1BJ, UK

^d Advanced Concepts Team, ESA-ESTEC, Keplerlaan 1, 2201 AZ Noordwijk, The Netherlands

ARTICLE INFO

Article history:

Received 2 November 2009

Received in revised form

12 January 2010

Accepted 31 January 2010

Keywords:

Inkjet technology

Micropumps

MEMS

Fuel injectors

Bipropellant rocket engines

ABSTRACT

Control over drop size distributions, injection rates, and geometrical distribution of fuel and oxidizer sprays in bi-propellant rocket engines has the potential to produce more efficient, more stable, less polluting rocket engines. This control also offers the potential of an engine that can be throttled, working efficiently over a wide range of output thrusts. Inkjet printing technologies, MEMS fuel atomizers, and piezoelectric injectors similar in concept to those used in diesel engines are considered for their potential to yield a new, more active injection scheme for a rocket engine. Inkjets are found to be unable to pump at sufficient pressures, and have possibly dangerous failure modes. Active injection is found to be feasible if high pressure drop along the injector plate is used. A conceptual design is presented and its basic behavior assessed.

© 2010 Elsevier Ltd. All rights reserved.

1. Introduction

The injectors in a chemical rocket motor are key in determining the efficiency of the reactions within the combustion chamber, ultimately affecting the performance of the motor. Critical to achieving good performance is the atomization process, whereby the propellant and oxidizer are transformed into small droplets; the size of these droplets is one of the factors that determine the mixing process and evaporation rates, which have a profound influence on the combustion reactions.

The basic function of the injector in a bipropellant liquid rocket is to atomize and mix the fuel with the oxidizer to produce efficient and stable combustion that will produce the required thrust without endangering hardware durability. Currently, most bipropellant rockets and hybrid rockets use small orifices in the injector plate,

which takes the form of a perforated disk at the head of the combustion chamber. To achieve high combustion performance and stable operation without affecting injector and thrust chamber durability requires proper selection and design specification of the entire flow-system geometry, which consists of the total element pattern, the individual orifice geometry and the flow system upstream of the orifices. The spray distributions (i.e. mass, mixture ratio and drop size distributions) are specified by the design of the complete flow-system geometry.

To arrive at the specification of the mixing and propellant drop size levels in the combustion chamber, combustion models are used and the results of these combustion model programs and experiments, have shown that combustion performance is highly dependent on the propellant spray distributions; high efficiency requires uniform mixture-ratio distribution, initial drop size consistent with the chamber geometry and operating conditions, and a uniform mass distribution.

The local mixture ratio and mass distributions near the injector face or chamber walls and also the radial and

* Corresponding author.

E-mail addresses: coletti@soton.ac.uk (M. Coletti), sbg2@soton.ac.uk (S.B. Gabriel), cristina.bramanti@esa.int (C. Bramanti).

transverse flows produced by adverse distributions of the overall mass or mixture ratio can have a strong impact on hardware durability; high rates of chemical reactions or material erosion caused by impingement of highly reactive propellants on the chamber wall can cause catastrophic damage of the chamber.

Thus more control over drop size distributions, injection rates, and geometrical distribution of fuel and oxidizer sprays has the potential to produce more efficient, more stable, less polluting rocket engines. This control also offers the potential of an engine that can be throttled, working efficiently over a wide range of output thrusts.

A preliminary feasibility study on the application of different types of injectors, inspired by non-space technologies, in rocket engines have been preformed and will be presented in this paper. Inkjet printing technologies, MEMS fuel atomizers [1], and piezoelectric injectors similar in concept to those used in diesel engines have been evaluated for their potential to yield a new, more active injection scheme for rocket engines. Different design configurations will be proposed and their potential applications will be evaluated.

2. Inkjet fuel injection

In this section the possible injection modes inspired by inkjet technologies will be presented and their potential application in rocket engines will be discussed. The possible inkjet injection modes can be divided into:

- Continuous inkjet
- Drop-on-demand inkjet (DOD)
 - Thermal
 - Electrostatics
 - Piezoelectric
 - Bend mode
 - Push mode
 - Shear mode

After presenting the different inkjet technologies (A) the surface tension needed by these inkjets (B) and the fundamental inkjet performance limits (C) will be presented. The inkjet pumping characteristics will be determined and their performance will be compared with the requirements of a 4, 40 and 400 N rocket engine (D). From this comparison inkjet technology will be considered unsuitable for fuel injection in rocket engines.

2.1. Basic technologies

Inkjet technologies can be split into two fundamental types: continuous and drop-on-demand (DOD).

Continuous inkjet designs are used in high volume applications. In a typical system, ink is supplied under pressure, and passes through a nozzle. The nozzle is excited at a frequency that promotes break-up of the jet into droplets around twice the size of the nozzle. Electrostatic deflectors are often combined with the droplet generator to deflect droplets away from the paper

when printing is not required. The Rayleigh breakup mode (Section 3.1) causes the droplets formed by these devices to be similar in diameter to the nozzle; it should be noted that much more efficient atomization is possible: under high pressure or with impinging flows droplets can be much smaller than the nozzle diameter.

The electrostatically actuated atomizer (designed with pulse detonation engines in mind) presented by Nabity and Daily [1] could be compared to a continuous mode inkjet when working in its atomizing mode of operation (the device is described working in two distinct ways: as an atomizer and as a pump). In this mode fuel is forced through a nozzle (a slot nozzle in this case) by the pressure of the fuel itself. An electrostatically actuated membrane just inside the nozzle is used to excite a high frequency disturbance of the jet/sheet as it leaves the device, which promotes a more rapid atomization and smaller droplets. The device also makes use of a transverse air jet across the nozzle to promote atomization; it is not clear how well it would perform without this air. The device is also capable of acting as a self-aspirating pump; the arguments presented below for inkjets are equally valid for this design.

Drop-on-demand inkjets are used in the majority of printers. There are three major types, based on the form of actuation: thermal, electrostatic and piezoelectric inkjets. In all three types, ink is supplied at ambient pressure, and is kept from leaving the printer nozzle by surface tension. Thermal inkjets are the most common type used in household printers, followed by piezoelectric ones.

2.1.1. Thermal inkjets

In a basic thermal inkjet (invented 1979, by Endo et al. [2] of Canon) water based ink is superheated by applying a current pulse of a few microseconds to an electrical heater located very close to the nozzle. A bubble forms very rapidly and pushes out a droplet. As the heat in the bubble is exhausted the bubble collapses and more ink is drawn in from the reservoir. The whole cycle occurs very rapidly—of the order of tens of microseconds.

An example of a thermal inkjet is the print-head of the Cannon i950 photo printer, which has 3072 nozzles, each capable of ejecting droplets of volume 2pL (corresponding to a droplet diameter of 16 μm) at a rate of 24 kHz. This represents a maximum flow rate of 0.15 ml/s. Thus it can be seen that to achieve the ~10–15 ml/s fuel flow required for a typical 40 N thruster we would need about 100 such print-heads. The large power consumption of thermal inkjets is the real obstacle to their use as fuel injectors: Chen and Wise [3] reports a typical energy of 11.5 μJ per droplet (of volume 34pl), which corresponds to a power consumption of over 4000 W for the fuel flow required for a 40 N thruster: This is clearly impractical, and thermal inkjets will not be considered further.

2.1.2. Electrostatic inkjets

Fig. 1 shows the principle of operation of an electrostatically actuated inkjet such as that described by Kamisuki et al. [4]. Electrostatic inkjet designs are capable of similar volume pumping rates to piezoelectric designs. The maximum pressure that an electrostatically

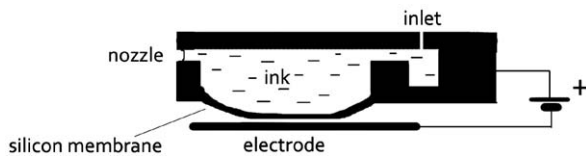


Fig. 1. Principle of operation of electrostatically actuated inkjet.

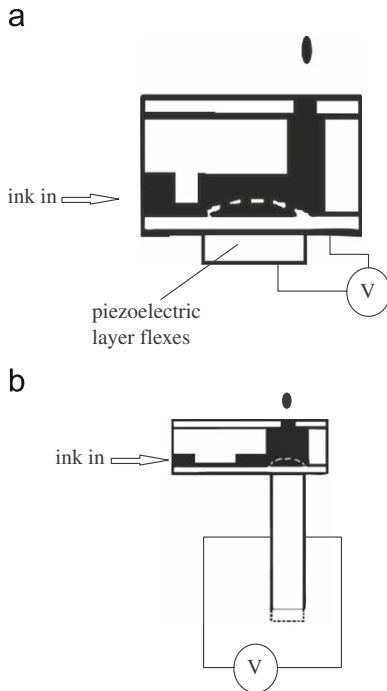


Fig. 2. Piezoelectric inkjet configurations—(a) bend-mode and (b) push-mode.

actuated membrane can generate is given by

$$P = \frac{\epsilon V^2}{2s^2} \quad (1)$$

where ϵ is the permittivity of the medium separating the plates, s the distance between the plate, and V the potential difference between them [5]. For example to produce an initial pressure (driver force per unit diaphragm area) of 1 bar from an electrostatic actuator acting in a vacuum requires a voltage/separation distance ratio of $150 \text{ V } \mu\text{m}^{-1}$. The silicon dioxide layer often used to separate the electrodes of electrostatic actuators has dielectric breakdown strength of $800\text{--}1000 \text{ V } \mu\text{m}^{-1}$. Allowing for some additional initial electrode separation, this results in a typical maximum initial pressure of around 4 bar.

2.1.3. Piezoelectric inkjets

Piezoelectric inkjets can be divided into three main categories according to the piezoelectric actuation mode: push, bend and shear; the first two are illustrated in Fig. 2. All rely on the deformation of the piezoelectric element to push out a droplet from the nozzle, and all three types have been used in commercial designs.

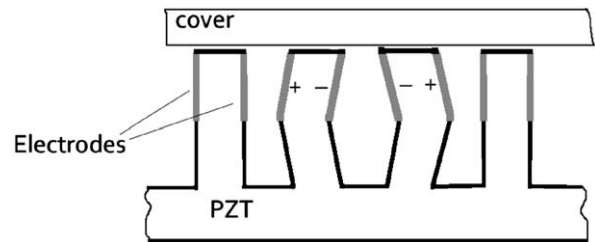


Fig. 3. Shear-mode inkjet design—applied voltage causes channel to widen.

The push-mode inkjet uses a PZT rod to push out the ink. In practice a thin membrane is placed between the rod and the ink to prevent interaction. In the bend-mode inkjet a piezoelectric layer is adhered to a thin steel or silicon membrane. When the piezoelectric layer is actuated it expands laterally, and in the manner of a uni-morph the resulting difference in strain between the piezoelectric and membrane causes the membrane to deflect either up or down. A thinning of the channel towards the ink supply causes a net pumping action.

2.1.4. Shear mode inkjet

The shear-mode inkjet [6] shown in Fig. 3, has electrodes deposited on the upper half of both sides of the channel walls. The applied field is thus perpendicular to the direction of polarization, and causes the walls to shear sideways, and squeeze out an ink drop (shearing is one of the modes of displacement of a piezoelectric element).

The commercially produced shear-mode inkjet, Xaar's XJ128 produces drops of diameter $42 \mu\text{m}$ at a rate of 8 kHz and a velocity of 10 m/s. This is comparable to typical piezoelectric bend-mode and electrostatic designs. Its power consumption is much higher than a bend-mode design to pump enough fuel for a typical 40 N thruster, which would need approximately 300 W electrical power.

2.2. Surface tension

In inkjet printers surface tension prevents unwanted ink flow out of the nozzle, and also prevents net backflow. The ink reservoir of an inkjet printer is not pressurized, and the question here is whether the surface tension will be sufficient to prevent flow when used in conjunction with a combustion chamber and pressurized fuel tank.

It should also be noted that the meniscus of an inkjet usually retracts some distance (e.g. 3 nozzle diameters [7]) into the chamber of the inkjet. If in a rocket engine this drew some combusting gases into the inkjet, there is a danger of (potentially catastrophic) damage to the inkjet.

The pressure difference required to overcome surface tension is given [8] by

$$\Delta P = \frac{4\sigma}{d} \quad (2)$$

where σ is the coefficient of surface tension and d the diameter of the nozzle. Fig. 4 shows the ΔP required to push droplets of MMH and NTO fuels through a variety of

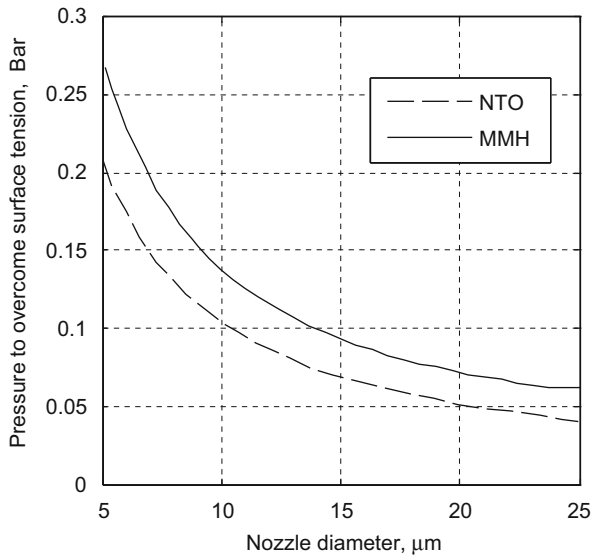


Fig. 4. Graph showing pressure required to overcome surface tension at various nozzle sizes.

nozzle sizes as calculated by the equation. It can be seen that at typical nozzle sizes of 20 μm or more any pressure difference above 0.06 bar would cause fuel to flow in or out of the nozzle.

This has several consequences:

- If fuel pressure was greater than the chamber pressure, as in a conventional rocket engine, then fuel would flow whether the inkjet was actuated or not, and uncontrolled jet of fuel would emerge from the nozzle.
- If fuel pressure was lower than chamber pressure, then to prevent backflow valves would be needed to isolate any injectors that were not being actuated. This would add a degree of complexity to an inkjet injector design, but is feasible as integrated microvalves are a continuing area of study for several research groups [9]. The failure of such valves could be catastrophic, with combustion products entering the fuel lines. It will be shown below, however, that inkjets are not capable of supplying sufficient pressure to operate in this configuration.
- Trying to match fuel pressure to combustion chamber pressure would be a complex way to ease these problems. However, fluctuations in chamber pressure are allowed for in conventional designs. If the magnitude of these fluctuations was bigger than the surface tension then either case (a) or (b) would happen. In the section that follows we will assess what level of fluctuations a piezoelectric actuator could accommodate.

2.3. Fundamental inkjet limits

The physics of how inkjets are actuated places some upper limits on their flow rate and maximum back-pressure.

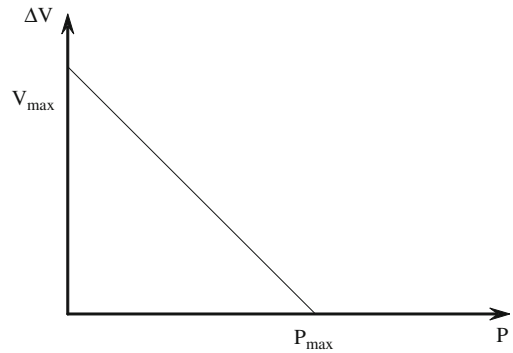


Fig. 5. Typical micropump characteristics.

2.3.1. Push-mode actuation

When a voltage is applied to a block of piezoelectric material there will be a displacement. When this displacement is blocked, a force will develop, the so-called blocking force [10]. The relationship of volume displacement to pressure applied is shown in Fig. 5, and it shows that the maximum displacement is only achieved if there is no pressure applied to the actuator face. If the actuator is to be used in a pump, the blocking pressure must be much larger than the pressure difference that the pump is required to work against; otherwise there will be a corresponding decrease in the pumped volume.

The stroke volume, ΔV_{MAX} , of a piezoelectric cylinder expanding along its axis is given by [10]

$$\Delta V_{MAX} = d_{33}AhE \quad (3)$$

where d_{33} is a piezoelectric coefficient, A the area of the top face, and E the applied electric field.

The blocking pressure, P_{max} , is given by

$$P_{max} = \frac{d_{33}E}{s_{33}} \quad (4)$$

where s_{33} is the compliance of the piezoelectric disc, and h its thickness. It should be noted that the stroke volume is proportional to the volume of the actuator, and that neither it, nor the blocking pressure are affected by the geometry of the actuator.

For example: a PXE-5 cylinder 10 mm in diameter and 1 mm thick, to which a 300 V voltage is applied, results in a blocking pressure of 65 bar and volume displacement of $9.18 \times 10^{-3} \text{ mm}^3$.

2.3.2. Bend-mode actuation

Bend-mode or membrane actuators produce a higher stroke volume. The membrane effectively amplifies the small lateral movements of the piezoelectric element into a much larger deflection of the membrane.

The stroke volume versus pressure graph is still of the form shown in Fig. 5. For the case of a circular membrane composed of two PZT 5A piezoelectric elements (a bi-morph), the stroke volume can be approximated as [10]

$$\Delta V = 2 \times 10^{-11} \frac{d^4}{h} E \quad (5)$$

where d is the diameter of the membrane, and h the total thickness (in meters). The blocking pressure is

$$P_{\max} \approx 4 \frac{h^2}{d^3} E \quad (6)$$

For example: a PZT 5A bimorph of total thickness 0.6 mm, and diameter 25 mm, actuated at a voltage of 150V, which gives a stroke volume of 6.5 mm³ and a blocking pressure of 0.5 bar. We have traded-off blocking pressure for stroke volume.

2.4. Inkjet characteristics required for a rocket engine

We will now determine what flow rates and maximum pressures an inkjet needs in order to inject fuel into a rocket engine. The estimates in this section are quite loose, but it will be seen that even if they varied by an order of magnitude the resulting evaluation of feasibility will be unchanged.

The total mass flow rates can be calculated as

$$\dot{m} = \frac{T}{g \cdot I_{SP}} \quad (7)$$

For a bipropellant MMH/NTO system I_{SP} is approximately 300 s. Table 1 lists the results for a range of thrusts. It also shows the self-pumping rate (flow normalized by total inkjet volume) required, given a certain acceptable total inkjet volume. This figure allows us to evaluate whether inkjets can pump suitable volumes of fuel without worrying about how many devices are required. Note that the acceptable volumes have been chosen to give the same normalized flow rate for each example, this makes comparison simpler.

The estimated maximum volumes take no account of the space required for plumbing to supply fuel to each inkjet or how to direct the output into a combustion chamber. The figures given are meant to form a reasonable upper bound.

For a given actuator stroke volume and blocking pressure, we wish to determine the characteristics of an inkjet using this element. An important feature of an inkjet, in contrast with many (but not all) micropumps, is that it has no check valves. There is a small directional dependence of the fluidic resistance of the inlet and outlet nozzles (a result of flow separation), which means that overall there is a net pumping action. A more detailed description can be found in Olsson et al. [11].

The ratio of flow rate through the nozzle to flow rate through the diffuser in each mode is typically of the order 4:3, and often much less [12,13]. Thus, the maximum droplet volume of an inkjet will be modeled here as one quarter of the displacement volume of the actuator. Similarly the blocking pressure of the pump (the pressure

that applied between outlet and inlet will reduce the net flow to zero) will be approximated as one quarter of the blocking pressure of the actuator [13].

To find the minimum blocking pressure that an inkjet would be required to operate at, we consider a system where the fuel pressure is maintained close to the combustion chamber pressure (see Section 4.1 above). Existing designs make allowance for pressure fluctuations in the chamber of the order of 10%, e.g. 0.8 bar for an EADS 22 N bipropellant thruster. In order that the flow rate is not significantly reduced by the back pressure (and also so that pressure fluctuations do not cause feedback and instabilities) we propose a blocking pressure of 8 bar. This pressure rules out the use of electrostatic inkjet designs in this case (see above).

Fig. 6 plots the required blocking pressure and normalized flow rates, comparing it with the predicted limits of inkjets calculated above. The lines in Fig. 6 show (in addition to results from the following section) the characteristics of inkjets that could be produced from both push-mode and membrane actuators. The y-axis shows the maximum flow-rate divided by total device volume (units: min⁻¹). This is sometimes called the self-pumping rate, and a value of, say, 10 on this axis would show that an inkjet could pump 10 times its own volume of liquid in each minute. The maximum flow rates have been calculated using an actuation frequency of 10 kHz—pumping above this frequency is rarely possible due to inertial effects. The push-mode actuator is plotted as a point, since its characteristics are determined solely

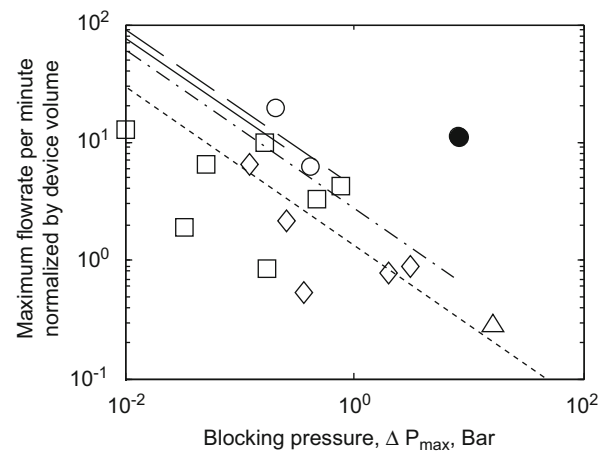


Fig. 6. Rocket requirements compared to ideal and actual micropump performance. ●=rocket engine requirement, Δ=push mode, ○=inkjet, □=piezo micropump valveless, ◇=piezo micropumps with valve, dotted line=10 m membrane, dash-dot line=100 m, dash-dash line=1 mm and solid line=3 mm.

Table 1
Fuel flow rates required for rocket engines.

Engine Thrust, N	4	40	400
v , Total fuel flow (cm ³ /min)	75	750	7500
V , Estimated maximum practical volume (cm ³)	1.9 × 1.9 × 1.9	4 × 4 × 4	8.6 × 8.6 × 8.6
Normalized flow rate \dot{v} (min ⁻¹)	11.1	11.1	11.1

by material properties (PZT-5A is used here). The device volume for the push mode inkjet has been assumed equal to the actuator volume. To calculate the device volume for the membrane inkjet a device height of 2 mm for the chamber walls plus the thickness of the membrane has been assumed. A maximum field strength of 300 V/m has been used [10].

Each line on the graph corresponds to a single membrane thickness over a range of diameters. It can be seen that (under the simple approximations used here) there is an optimum membrane thickness of around 1 mm, and that by varying its diameter, a range of different volume/pressure combinations can be obtained. The lines are only plotted for reasonable thickness to diameter ratios of 0.1 or less. Membranes thicker than this would cease to conform to the approximations given above, and perform less well than the approximations might suggest.

The graph also shows data from a selection of micropumps described in the literature [5], and includes data for a range of actuator types, including some devices with valves. There are only two points for inkjets as the blocking pressure of an inkjet is rarely measured: the one with the lower blocking pressure is a shear-mode inkjet [6], and the other an electrostatically actuated one [7].

It can be seen that although some pump designs can produce sufficient flow, the blocking pressure at these flow rates is more than an order of magnitude below that required.

Thus, even if significant efforts were put into developing a high pressure inkjet or micropump, it is unlikely that a design with sufficient flow rate could be produced.

We can then conclude that inkjets are not suitable for use as rocket fuel injectors where significant pressure fluctuations exist in the combustion chamber. There is a possibility that the reduced droplet sizes and an active control system might reduce the pressure fluctuations; Inkjets can supply sufficient flow rates, and we estimate that if the pressure fluctuations could be reduced to less than 0.05 bar (that is 0.6% of a typical 8 bar chamber pressure), then inkjets could supply the required fuel. This may well be unrealizable.

The arguments presented above are also valid for micropumps, except that designs with valves would not suffer the pressure and volume loss caused by not having them; this would be offset, however, by a much reduced pumping frequency, so micropumps would also likely to be unsuitable in this application. Micropumps with check-valves also (e.g. Li et al. in Nyugen et al. [14]) devote considerable space to the valves, increasing the pump volume. Microfabricated check-valves are also prone to clogging and can exhibit significant pressure losses [12], and Gravesen et al. [15] notes, “long-term problems related to sedimentation or wear must be foreseen.”

3. Active injection

The application in rocket engines of injectors, comparable to those found in diesel engines, has been evaluated

and will be discussed in the present section. In this kind of injectors the nozzle size and pressure are defined in order to achieve a high degree of atomization. The fine atomization and degree of control afforded by active injection makes it an attractive alternative for producing rocket motors that are more efficient, cleaner, allowing for a control in real time of the combustion instabilities and tractability range.

Diesel injectors were first produced in the 1920s and have evolved considerably since then. The first common rail injection system was produced [16] in 1997. This configuration permits full electronic control of the injection event. A fuel pump operates continuously, pressurizing fuel to typically 1000 bar (recent designs operate at even higher pressures) and feeds it into the common rail where it is held ready for injection. Individual injectors feed fuel directly into the engine's combustion chambers. The injectors are controlled electronically, so the quantity of fuel injected is independent of engine or pump speed, and can be fired at any point in the cycle. Piezoelectric transducers have replaced electromagnetic actuators on many more recent designs. The higher force and quicker response time of a piezoelectric transducer means that the valve can be opened and shut more quickly. This result in a higher average velocity and hence smaller droplet sizes [17], and also permits more precisely metered quantities of fuel. Thus piezoelectric injectors can produce cleaner, more efficient engines. The working pressure of diesel engines is quite different from the rocket engines and in the analysis presented below it will be assessed whether the injectors inspired by diesel engines can be used in rockets.

Changing the size and distribution of droplets would have significant effects on the combustion in the chamber of a rocket engine. In a plain orifice diesel injector under high pressure the droplets can be very much smaller than the injector nozzle diameter—droplet sizes can be less than 0.1 of the nozzle diameter [18]. Compare this to typical ratios of 0.2 to 0.4 for impinging injectors in a rocket engine (as described by Santoro and Anderson [19]). Santoro comments on several factors affecting stability in impinging injectors, noting: (a) that reducing droplet size will bring combustion closer to the injector face and hence reduce stability by coupling the combustion more closely to the injector dynamics; (b) that “it is reasonable to expect that stability will be enhanced if there is a wide distribution of drop sizes because any present effects of resonant burning can be essentially neutralized by different-sized drops that release most of their chemical energy out of phase with the drops that are burning in resonance with pressure oscillations.”; and (c) that “The frequency with which periodic surface waves and ligament structures are formed have a marked similarity to the highest possible combustion instability frequency as predicted by the stability correlation.”. It is thus uncertain what effect the use of active injection will have on combustion stability: points (a) and (b) suggest that we risk increased combustion instability, but (c) suggests that by working in the atomization break-up mode (see below) there may be less excitation of instability modes (though care must be taken not to

actuate injectors at frequencies that would excite instability modes).

Another consequence of reducing droplet sizes would be that as the combustion area moved closer to the injector face, the temperature stresses on the injectors would be increased.

3.1. Applicability to rockets

The applicability of diesel injectors to rocket engines mainly depends on whether the injector propellant pressure can be reduced to a value that can be achieved in a rocket while maintaining sufficient flow and atomization, and also whether existing technology could be used to implement such a system.

If fuel of density ρ_L is forced through a nozzle by a pressure differential, ΔP , using the Bernoulli equation and introducing a coefficient to take into account the behavior

of a real fluid (C_D) the velocity of the resulting jet can be approximated as [20]

$$v = C_D \sqrt{\frac{2\Delta P}{\rho_L}} \tag{8}$$

where C_D is the discharge coefficient (see Lefebvre [20] for the effect of Reynolds number and orifice geometry on C_D). The break-up of a jet exiting from a plain orifice can take one of several modes depending (ignoring the effect of nozzle geometries and upstream flow characteristics) on the velocity of the jet, the properties of the fuel and the pressure; this is illustrated in Fig. 7. At low velocities the Rayleigh mode, caused by the growth of unstable perturbations of the jet, produces drops approximately 1.9 times the size of the orifice. As the velocity is increased interactions with the surrounding gas produce the first, and second wind-induced modes and finally the atomization mode is reached, which is also much influenced by cavitation and turbulence in the initial jet. In the first wind-induced mode the droplet size is of the same order as the orifice, while in the subsequent modes the droplet sizes are very much smaller. If such an orifice were to be used in a rocket injector, we would want to be in the second-wind induced or atomization modes.

Lin and Reitz [23] have suggested a scheme for determining which break-up mode is likely for a given system

- Break-up mode 1: The Rayleigh break-up region: $W_{el} < 8$ and $W_{eG} > 0.4$ or $1.2 + 3.41 Z^{0.9}$
- Break-up mode 2: The first wind-induced region: $1.2 + 3.41 Z^{0.9} < W_{eG} < 13$
- Break-up mode 3: The second wind-induced region: $13 < W_{eG} < 40.3$
- Break-up mode 4: Atomization region: $W_{eG} > 40.3$.

Various combinations of fuel pressure, nozzle diameter and degree of atomization have been derived. Table 2 lists the fuel properties used in the calculations. The discharge coefficient, C_D , was approximated using the data given in Lefebvre [20], which relates it to Reynolds number and nozzle geometry (a nozzle width to length ratio of 0.25 was used).

Fig. 8 shows the results for a range of pressures for an orifice diameter of 100 μm . The vertical axis indicates the relative pressure drop across the injectors while the horizontal axis indicates the chamber pressure in bars. The markers indicate the transition between break-up

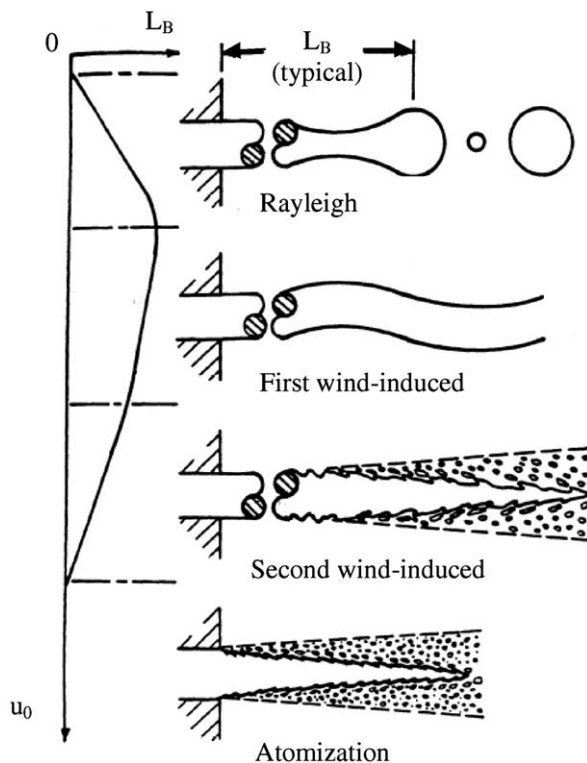


Fig. 7. Mechanical jet break-up regimes (from Faeth [22]).

Table 2
Fuel properties.

Fuel	Dynamic viscosity (kg/(ms))	Density (kg/m ³)	Surface tension (kg/s ²)
MMH	7.71×10^{-4}	8.78×10^2	3.43×10^{-2}
NTO	4.10×10^{-4}	1.44×10^3	2.63×10^{-2}
LOX	2.2×10^{-4}	1.15×10^3	2×10^{-2}
H2	1×10^{-5}	71	0.2×10^{-2}
RP1	2.4×10^{-2}	8.3×10^2	2.8×10^{-2}

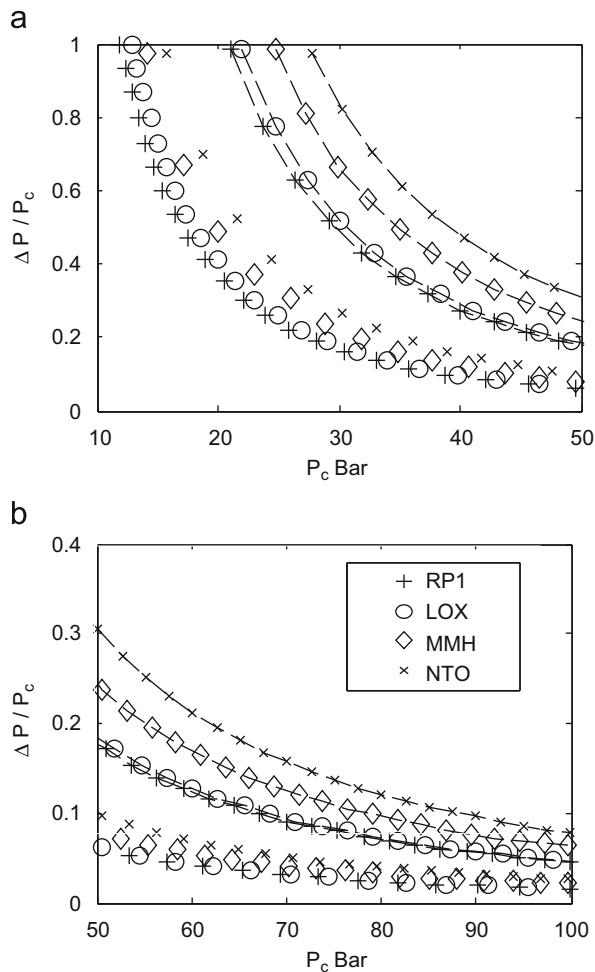


Fig. 8. Break-up modes for different pressures and pressure drops with an orifice diameter $D=100\ \mu\text{m}$. (a) Chamber pressure from 10 up to 50 bar and (b) chamber pressures from 50 to 100 bar.

regions 2 and 3, while the dashed-markers lines indicate the transition between modes 3 and 4.

From Fig. 8, it can be pointed out that, for example, to operate in break-up region 4 (the one providing the smallest droplet size), a chamber pressure between 47 and 62 bars is required, considering a pressure drop across the injectors of about 20%. If the diameter of the orifices is $50\ \mu\text{m}$ and $200\ \mu\text{m}$, the pressure ranges become 65–88 bars and 33–44 bars, respectively.

3.2. Active injection—a design idea

This section presents a proposed design that demonstrates a possible configuration for an active injection system for the 50 kN bipropellant thruster. Only basic calculations have been performed to assess its performance—the in depth analysis and refinement of this design will be the subject of future work. The use of cryogenic propellants has not been taken into account since few data exist relative to the capability of PZT to

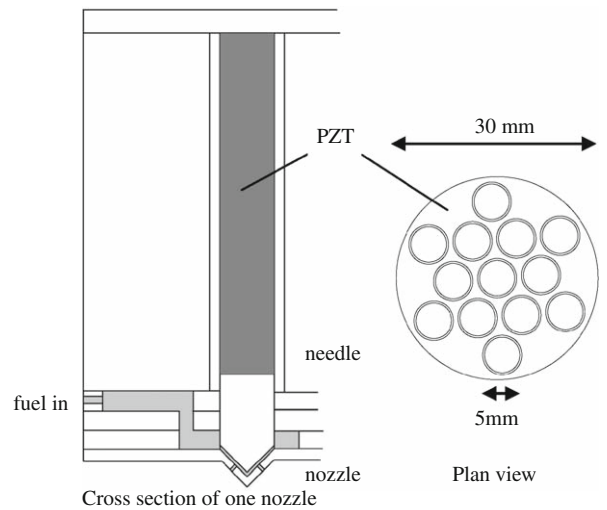


Fig. 9. Proposed Active Injector system (not to scale).

Table 3
Active injector design parameters.

	MMH	NTO
Total thrust	50 kN	
Chamber Pressure	60 bar	
Pressure drop	12 bar (20% of chamber pressure)	
Nozzle diameter	100 μm	
Fuel velocity (m/s)	42	33
Number of nozzles	10,000	5000
Nozzles per injector	10	10
Number of injectors	1000	500
Maximum mass flow rate (kg/s)	11.6	7.5
Break-up mode (see above)	Second-wind induced/atomization	
Droplet diameters, SMD	Further study required: approx. 30 μm	
Injector plate diameter	~0.5 m	

work at cryogenic temperatures even though work by Park et al. [24] has demonstrated a PZT actuated microvalve that operates down to 40 K.

The design is shown in Fig. 9, and the key properties of the design are listed in Table 3. It comprises a number of piezoelectrically actuated injectors, each injector having a number of nozzles. The overall diameter of the system and of each injector as marked on the figure is only an estimate of what might be feasible. Since the pressures involved are much lower than those found in a diesel engine, the piezoelectric actuators act directly on the nozzle needle. Using a similar, but longer, stacked piezoelectric actuator than the one described by Yang et al. [21], a stroke distance on $50\ \mu\text{m}$ will occur at an actuation voltage of 60 V for an actuator length of 50 mm. Further work is required to determine if this is sufficient to maintain the predicted flow rates, and also to ensure that the actuator supplies sufficient seating force to prevent leakage.

The number of fuel and oxidizer nozzles has been tailored to provide close to the optimum oxidizer to fuel

mass ratio of 1.6 at full thrust. Since this scheme provides the possibility of active control, the total number of nozzles supplied in the design exceeds the minimum number required so that even at maximum thrust there is the possibility of tailoring the spatial distribution of the oxidizer/fuel ratio.

The power consumption can be estimated using data presented by Yang. To hold open all 1500 injectors would consume about 45 W (this is dissipated through leakage currents in the actuators). Additional power is consumed to change the state of the actuators. It is envisaged that in most modes of operation, most injectors would be held in a steady state most of the time (nozzles can be held half open at no extra power cost), with some small adjustments for control purposes.

Piezoelectric actuators have a very fast response time, and this opens up the possibility of using active control to reduce combustion instabilities in the combustion chamber. Further study based on computational fluid dynamics or experiment would be required to form an accurate prediction of the distribution of droplet sizes, and combustion dynamics. Further investigation is needed to evaluate whether incorporating active injectors would increase the performance of a rocket sufficiently to justify the additional complexity and weight. The main advantages would be very good throttling control (varying the mass flow rate and hence the thrust from zero flow up to the maximum level), through adjusting the duty cycle, and the possibility of active instability control. Increased efficiency is also likely due to smaller droplets.

4. Conclusions and future works

Inkjets have been assessed as a possible method of injecting fuel into a bipropellant rocket engine. It was found that the surface tension effects (that normally prevent unwanted ink escaping) can only resist fuel pressures differences of the order of 0.05 bar for typical nozzle sizes. This means that unless the fuel pressure could be closely matched to the combustion chamber and fluctuations in chamber pressure were much reduced there would be a need for valves. Considering the physics of devices, the actuation technologies (piezoelectric, electrostatic; thermal-bubble consumes too much power) place limits on the maximum flow rates and blocking pressures of the inkjets. It was found that while inkjets are capable of suitable flow rates, none of the actuation technologies can also supply sufficient pressure. The only situation in which inkjets can generate sufficient pressure is if fuel pressure matched chamber pressure, and the chamber pressure fluctuations (from combustion instabilities) were reduced to less than 0.05 bar. The authors know of no actuation technologies under development that would change this situation in the foreseeable future. Additionally, during the intake part of the inkjets' cycle combustion chamber gases would be drawn into the inkjet body, with the risk of serious damage to the inkjet.

We can then conclude that inkjet injection technology is not applicable to chemical rocket motors.

Injectors inspired by diesel injectors for car engines were assessed. The precise control over the injectors means that this type of technology offers the possibility of full throttling control, varying the mass flow rate (hence the thrust) from zero up to its maximum value, along with increased efficiency and with the possibility, being able to vary the mass flow rate in every injector, to perform active control of combustion instabilities. A design concept has been proposed, along with some basic calculations to show its expected performance. Much further work is required to investigate this design fully. In particular future studies will have to be focused on

- modelling flow through the entire design, checking whether this design provides sufficient opening distance, and sufficient seating force for leak-free operation.
- Experiments and further design to ensure reliable injector operation, in particular: chemical isolation of PZT from fuels, possible lubrication additive to fuel, and investigation of clogging and filtration.
- Using experiments or modelling to determine the distribution of droplet sizes and droplet penetration the injectors would produce.
- Using experiments or modelling to assess the effects of droplet size changes and other parameters on dwell times of unburnt fuel, mixing, combustion stability, etc.
- Thermal modelling to ensure materials are not overstressed.

Overall system modelling to determine appropriate layout of injectors to provide required functionality over a range of output thrusts, and effective active control will also be needed.

Acknowledgments

This project was funded by the European Space Agency through the Ariadna programme, study no.: AO/1-5180/06/NL/HE.

Appendix A. Nomenclature

A	Area
C_D	discharge coefficient
d	Diameter
d_{33}	piezoelectric coefficient
ϵ	Permittivity
E	electric field strength
G	gravitational acceleration
h	thickness
I_{sp}	specific impulse
\dot{m}	rate of mass flow
P	pressure
P_{max}	blocking pressure
ΔP	pressure drop across a device
ρ_L	liquid density
ρ_g	gas density
s	distance
s_{33}	compliance in the direction of polarization
σ	coefficient of surface tension
T	thrust

V	potential difference and volume
v	velocity
ΔV	change in volume
W_{eG}	weber number for gas, $\rho_G v^2 D / \sigma$
W_{eL}	weber number for liquid, $\rho_L v^2 D / \sigma$
Z	ohnesorge number, $\mu / \sqrt{\rho_L \sigma D}$

References

- [1] J. Nability, J. Daily, A MEMS fuel atomizer for advanced engines, in: Proceedings of the Conference on Micro-Nano-Technologies, Monterey, California, 2004.
- [2] I. Endo, Y. Sato, S. Saito, T. Nakagiri, S. Ohno, (Canon), Liquid jet recording process and apparatus there for, Great Britain Patent 2007162, 1979.
- [3] J.K. Chen, K.D. Wise, A high-resolution silicon monolithic nozzle array for inkjet printing, IEEE Transactions on Electron Devices 44 (9) (1997) 1401–1409.
- [4] S. Kamisuki, T. Hagata, C. Tezuka, Y. Nose, M. Fujii, M. Atobe, A low power, small, electrostatically driven commercial inkjet head, MEMS 98, Heidelberg, Germany, 1998.
- [5] D.J. Laser, J.G. Santiago, A review of micropumps, Journal of Micromechanics and Microengineering 14 (6) (2004) R35–R64.
- [6] J. Brunahl, Physics of piezoelectric shear mode inkjet actuators, Ph.D. Thesis, Royal Institute of Technology, Stockholm, 2003.
- [7] C.D. Meinhardt, H.S. Zhang, The flow structure inside a microfabricated inkjet printhead, Journal of Microelectromechanical Systems 9 (1) (2000) 67–75.
- [8] F.M. White, Fluid Mechanics, 3rd ed, McGraw-Hill, New York, 1994.
- [9] J. Mueller, Review and applicability assessment of MEMS-based microvalve technologies for microspacecraft propulsion, micropropulsion for small spacecraft, in: M. Micci, A. Ketsdever (Eds.), Progress in Astronautics and Aeronautics, American Institute of Aeronautics and Astronautics, 2000, pp. 449–476.
- [10] Morgan Electro Ceramics, Piezoelectric ceramics properties and applications 2007.
- [11] A. Olsson, G. Stemme, E. Stemme, A valve-less planar fluid pump with 2 pump chambers, Sensors and Actuators A—Physical 47 (1–3) (1995) 549–556.
- [12] A. Olsson, P. Enoksson, G. Stemme, E. Stemme, Micromachined flat-walled valveless diffuser pumps, Journal of Microelectromechanical Systems 6 (2) (1997) 161–166.
- [13] M. Koch, Silicon micromachined pumps employing piezoelectric membrane actuation for microfluidic systems, Ph.D. Thesis, University of Southampton, 1997.
- [14] N.T. Nguyen, X.Y. Huang, T.K. Chuan, MEMS-micropumps: a review, Journal of Fluids Engineering—Transactions of the ASME 124 (2) (2002) 384–392.
- [15] P. Gravesen, J. Branebjerg, O.S. Jensen, Microfluidics—a review, Journal of Micromechanics and Microengineering 3 (1993) 168–182.
- [16] Bosch, Diesel-Engine Management, 3rd ed, Robert Bosch GmbH, Stuttgart, Germany, 2004.
- [17] S.W. Park, J.W. Kim, C.S. Lee, Effect of injector type on fuel-air mixture formation of high-speed diesel sprays, Proceedings of the Institution of Mechanical Engineers Part D—Journal of Automobile Engineering 220 (D5) (2006) 647–659.
- [18] C. Bae, J. Yu, J. Kang, J. Kong, K. Lee, Effect of Nozzle Geometry on the Common-Rail Diesel Spray, 2002.
- [19] R.J. Santoro, W.E. Anderson, Final Report on Combustion Instability Phenomena of Importance to Liquid Propellant Engines, Department of Mechanical Engineering and Propulsion Engineering Research Center, Pennsylvania State University, 1994.
- [20] A.H. Lefebvre, Atomization and Sprays, Hemisphere Publishing/Taylor & Francis, New York, 1989.
- [21] E.H. Yang, C. Lee, J. Mueller, T. George, Leak-tight piezoelectric microvalve for high-pressure gas micropropulsion, Journal of Microelectromechanical Systems 13 (5) (2004) 799–807.
- [22] G.M. Faeth, L.P. Hsiang, P.K. Wu, Structure and breakup properties of sprays, International Journal of Multiphase Flow 21 (1995) 99–127.
- [23] S.P. Lin, R.D. Reitz, Drop and spray formation from a liquid jet, Annual Review of Fluid Mechanics 30 (1998) 85–105.
- [24] J.M. Park et al., A piezoelectric microvalve for cryogenic applications, Journal of Micromechanics and Microengineering, 18 015023, 10pp doi:10.1088/0960-1317/18/1/015023.